Physical properties of $Fe_{80}P_{20}$ glass-carbon nanotubes composite

Y. B. LI*, B. Q. WEI, C. L. XU, J. LIANG, D. H. WU
*Department of Mechanical Engineering, Tsinghua University, Beijing 100084,
People's Republic of China*
E-mail: ybli@mail.cic.tsinghua.edu.cn

The $Fe_{80}P_{20}$ amorphous alloy and $Fe_{80}P_{20}$ amorphous alloy embedded with 1 and 2 wt % carbon nanotubes were fabricated by rapid solidification process and their non-isothermal differential scanning calorimetry (DSC) curves, hysteresis loops at room temperature and low-temperature electric resistivities and ac magnetic susceptibilities were measured respectively. The results indicate that the addition of nanotubes greatly enhance the thermal stability and the electric resistivity, but decrease the saturation magnetic moment, and $Fe_{80}P_{20}$ glass-2wt% nanotubes composite has an antiferromagnetic transition at about 180 k. © *1999 Kluwer Academic Publishers*

1. Introduction

Since carbon nanotubes (CNTs) were discovered by Iijima [1], lots of researches have been carried out to decide their structural characteristics and various properties. It has been well known that nanotubes have very interesting electric properties [2] and high mechanical properties [3]. A valuable application of CNTs in composite field has been highly evaluated because CNTs possess much higher modulus and hardness and have better stiffness than other carbon fibers [4]. It has been reported that the addition of CNTs in different matrixes do have some effective enhancement to the matrix properties, for example, a superconductor with embedded CNTs has enhanced flux pinning [5]. Amorphous alloys are interesting materials from a technological standpoint. They possess high corrosion resistance and attractive magnetic parameters. Ferromagnetic amorphous glasses are suitable for use in flux multipliers because of their extremely soft magnetic behavior and high resistivity [6]. The processing of a CNTs/Fe-P glass composite fabricated by "melt-spinning" rapid solidification (RS) method has been reported in a former letter [7]. In this paper, some physical properties of $Fe_{80}P_{20}$-CNTs composite, such as thermal stability, magnetization and electric resistivity, by contrasting to those of $Fe_{80}P_{20}$ amorphous alloy, will be introduced.

2. Experimental

The $Fe_{80}P_{20}$-2wt%CNTs, $Fe_{80}P_{20}$-1wt%CNTs and $Fe_{80}P_{20}$ alloy ribbons about 35 μm in thickness were fabricated respectively on a single-roller RS apparatus under argon atmosphere. The specific processing conditions refer to [7]. CNTs were prepared by catalytic pyrolysis method like that introduced in [8, 9].

The average diameter of fabricated CNTs was about 15 nm. The ribbons were examined by X-ray diffraction and selected area electron diffraction techniques, which proved the $Fe_{80}P_{20}$ matrixes were amorphous. The samples prepared by chemical thinning method were observed under a JEM-200CX transmission electron microscope (TEM). Three kinds of ribbons were annealed at 160 °C for 1 hour, then their M-H hysteresis loops at room temperature were measured on a Micromag TM2900 alternating gradient magnetometer. The resistivities of $Fe_{80}P_{20}$ amorphous ribbon and $Fe_{80}P_{20}$-2wt%CNTs ribbon below room temperature were measured by four-probe method respectively with liquid helium acting as cooling medium. In addition, their ac magnetic susceptibilities ($f = 314$ Hz) at low temperature were also measured. The thermal stability of fabricated ribbons were characterized by means of non-isothermal differential scanning calorimetry (DSC) technique. The continuous heating DSC experiments were carried out in a Perkin-Elmer DSC 7 apparatus, using dry argon as the purge gas. The samples, of about 3–4 mg weight, were heated up to 200 °C at a heating rate of 50 °C/min, then to 600 °C at a heating rate of 10 °C/min for all runs.

3. Results and discussions

The TEM images of $Fe_{80}P_{20}$-2wt%CNTs composite are shown in Fig. 1 from which nanotubes stretching out from $Fe_{80}P_{20}$ amorphous matrix can be seen. The observed nanotubes are as perfect as those used in the raw materials and most of them disperse in the matrix. A nanotube coated by Fe-P amorphous alloy at one end is indicated with an arrow in Fig. 1b, which implies the good wettability between nanotubes and Fe-P alloy

---

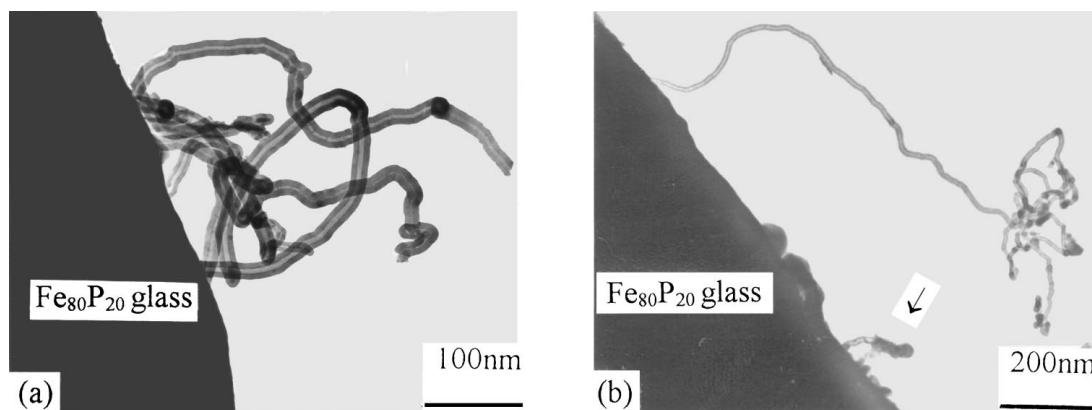* Author to whom all correspondence should be addressed.

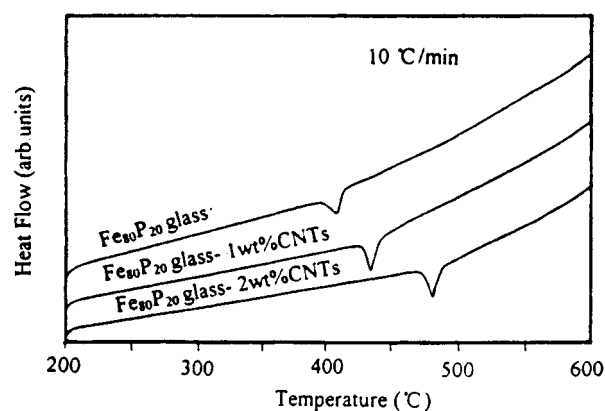*Figure 1* TEM micrographs of $Fe_{80}P_{20}$ glass-2wt%CNTs composite.

Figure 2 Non-isothermal DSC curves of the fabricated RS ribbons: (a) $Fe_{80}P_{20}$ glass; (b) $Fe_{80}P_{20}$ glass-1wt%CNTs; (c) $Fe_{80}P_{20}$ glass-2wt%CNTs.

matrix. It is believed that the choose of eutectic Fe-P alloy matrix and the short melt duration time are very important in keeping nanotubes survive the process. The dispersion of CNTs in the matrix and good wettability between CNTs and the matrix enable nanotubes act as an excellent reinforcer in Fe-P amorphous matrix.

Fig. 2 shows the non-isothermal DSC curves of the fabricated ribbons. Each of DSC curves display an individual peak respectively at a different temperature zone. The X-ray diffraction results of three annealed samples proved that Fe_3P and α-Fe phases were precipitated during their crystallization processes. The extended onset temperatures (T_e) and peak temperatures (T_p) of their crystallization processes are listed in Table I. The values in Table I confirm that the addition of 1 and 2wt% CNTs in the $Fe_{80}P_{20}$ glass matrix make the crystallization onset temperature increased by 34 and 80 °C respectively. The results allow us to conclude that the

TABLE I The onset temperature and peak temperature of non-isothermal crystallization process

Sample	T_e (°C)	T_p (°C)
$Fe_{80}P_{20}$ glass	395	407
$Fe_{80}P_{20}$ glass-1wt%CNTs	429	434
$Fe_{80}P_{20}$ glass-2wt%CNTs	475	479

addition of nanotubes can apparently enhance the thermal stability of the amorphous Fe-p matrix. From this effect we can infer that nanotubes in the matrix may retard the phosphorus element's long-range atomic rearrangements required for the precipitation of Fe_3P and α-Fe phases, which may result from that the "chaos" in the amorphous iron alloy matrix aroused by nanotubes make phosphorous atoms diffuse more difficultly. In addition, the large incompatibility between atomic spacing of nanotube and that of Fe_3P make it impossible for nanotube to act as an effective nucleating site for Fe_3P phase. The thermal stability of amorphous metallic alloy is a very important indicator for its application. The better thermal stability and high mechanical properties brought out by the addition of CNTs make the fabricated $Fe_{80}P_{20}$ glass-CNTs composites have a promising application.

Fig. 3 shows the hysteresis loop of $Fe_{80}P_{20}$-2wt%CNTs annealed at low temperature that was measured at room temperature. The other fabricated ribbons display the similar soft magnetic property. The saturation magnetic moment per unit mass (M_s) and coercive force (H_c) for three kinds of annealed ribbons are listed in Table II. It can be concluded that Ms greatly decrease with the content of CNTs increasing, for example, M_s is cut down by 30% from 244 to 165 emu/g when a volume fraction of 9% (2 wt %) CNTs are embedded in the Fe-P amorphous alloy. Nanotubes have a much smaller magnetic moment [10] than iron alloy at
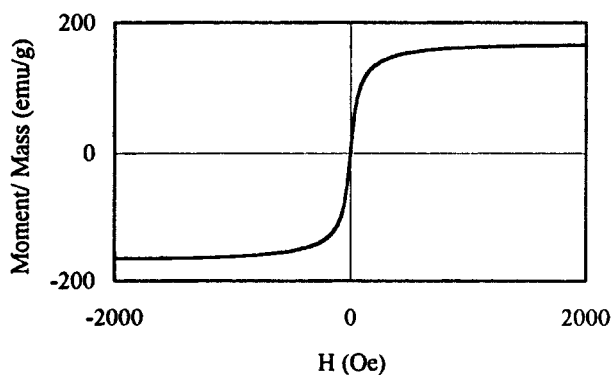

Figure 3 M-H hysteresis loop of $Fe_{80}P_{20}$ glass-2wt%CNTs at room temperature.

TABLE II The saturation magnetic moment and coercive force at room temperature

Sample	M_s (emu/g)	H_c (Oe)
$Fe_{80}P_{20}$ glass	244	0.65
$Fe_{80}P_{20}$ glass-1wt%CNTs	197	0.41
$Fe_{80}P_{20}$ glass-2wt%CNTs	165	0.35
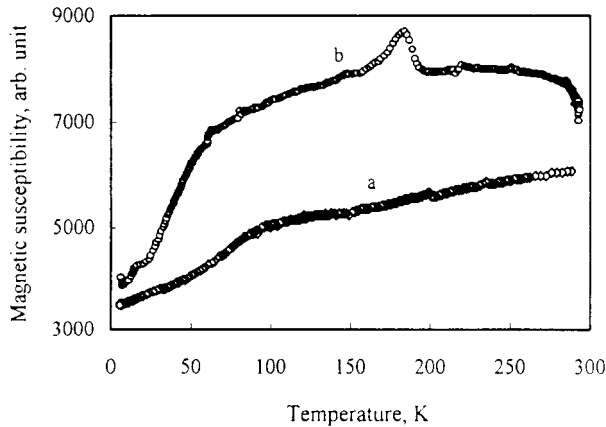
Figure 4 The low-temperature a.c. magnetic susceptibility curves: (a) $Fe_{80}P_{20}$ glass; (b) $Fe_{80}P_{20}$ glass-2wt%CNTs.

Figure 5 The low-temperature electric resistivity curves: (a) $Fe_{80}P_{20}$ glass; (b) $Fe_{80}P_{20}$ glass-2wt%CNTs.

room temperature, but according to the decrease in Ms only caused by CNTs occupying some volume of iron alloy, we can not completely account for the measured results. That is to say, we must consider that CNTs have a strong retarding effect on the development of magnetic domains or may change the shape of magnetic domains in Fe-P alloy.

Besides, we have measured the ac magnetic susceptibility of $Fe_{80}P_{20}$ glass and $Fe_{80}P_{20}$-2wt%CNTs at low temperatures which are shown in Fig. 4. An antiferromagnetic transition at 180 K for $Fe_{80}P_{20}$-2wt%CNTs can be seen, while $Fe_{80}P_{20}$ glass display a paramagnetic phenomenon at low temperature. According to Neel, there exist stacks of ferromagnetically ordered layers whose magnetization alternates from layer to layer in the antiferromagnetic material. In order to correctly interpret the antiferromagnetic phenomenon observed in $Fe_{80}P_{20}$-2wt%CNTs, further detections on the detailed structural characterization especially around nanotubes are needed to be done.

Fig. 5 shows the low-temperature resistivity of $Fe_{80}P_{20}$-2wt%CNTs and $Fe_{80}P_{20}$ glass. The curve of $Fe_{80}P_{20}$ amorphous alloy has a minimum resistivity at 25 K and above 25 K the resistivity increases linearly with the temperature increasing at a coefficient of resistivity-temperature (CRT $= 1/\rho \cdot d\rho/dT$, where ρ refers to resistivity) of about 3.2×10^{-4}, and ρ (270 K) is 193 $\mu\Omega$ cm. It can be seen from the resistivity-temperature curve of $Fe_{80}P_{20}$-2wt%CNTs that below 180 K the resistivity change little, which means CRT is near to zero, but above 180 K the resistivity decreases linearly with the temperature increasing which is characterized with a CRT of about -1.5×10^{-4} and its ρ (270 K) is 324 $\mu\Omega$ cm. It is known that CNTs can change from metallic to semiconducting when their diameters or helicities change, so the low-temperature re-
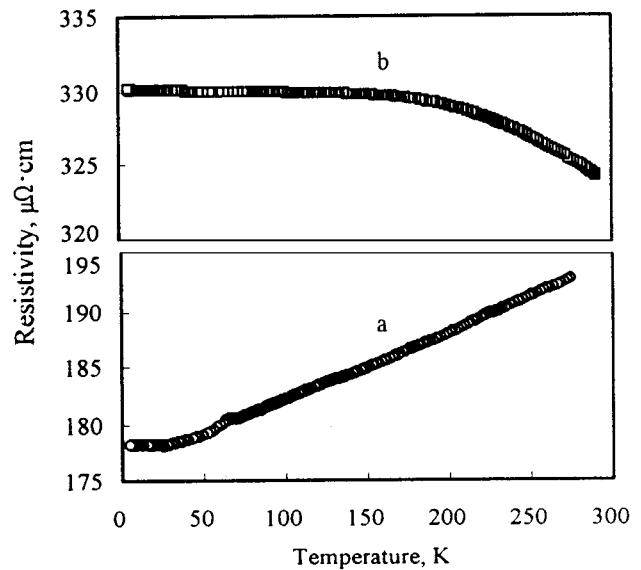
sistivity of bulk CNTs that obtained by a hot-pressing process were also measured. The fabricated CNTs have a high resistivity of the order of 10^{-4} Ω cm and a negative CRT at low temperatures, which is consistent with the results of some individual multi-shell nanotubes [11]. It can be concluded from above that CNTs dispersing in the amorphous alloy matrix play a critical influence on the transport property of fabricated composite, which means the addition of CNTs in the Fe-P amorphous alloy greatly enhance the electric resistivity and change CRT feature. From above we know there is an antiferromagnetic transition and a CRT change at 180 K for $Fe_{80}P_{20}$-2wt%CNTs, which may result from the microstructural changes in the composite at low temperature. Because the high resistivity and negative CRT are the valuable properties for the amorphous alloy, the $Fe_{80}P_{20}$-CNTs composite may be applied to some engineering products. To successfully explain physical properties of $Fe_{80}P_{20}$-CNTs composite, further researches about its microstructural changes at different conditions are to be carried out.

4. Conclusion
The addition of 2 wt % nanotubes in the $Fe_{80}P_{20}$ glass enhance the crystallization onset temperature by 80 °C and increase the low-temperature electric resistivity by about 70%, but decrease the magnetization by about 30%. In summary, $Fe_{80}P_{20}$ glass-CNTs composite exhibit better thermal stability and much greater low-temperature resistivity than $Fe_{80}P_{20}$ amorphous alloy, which enable $Fe_{80}P_{20}$ glass-CNTs composite become a valuable soft magnetic material although its magnetization is lower than that of $Fe_{80}P_{20}$ glass.

References

1. S. IIJIMA, *Nature* **354** (1991) 56.
2. M. S. DRESSELHAUS, G. DRESSELHAUS and R. SAITO, *ibid.* **33** (1995) 883.
3. R. S. RUOFF and D. C. LORENTS, *Carbon* **33** (1995) 925.
4. M. M. J. TREACY, T. W. EBBESEN and J. M. GIBSON, *Nature* **381** (1996) 678.
5. K. FOSSHEIM, E. D. TUSET, T. W. EBBESEN, M. M. J. TREACY and J. SCHWARTZ, *Physica C* **248** (1995) 195.
6. M. P. TRUJILLO, A. OROZCO, M. CASAS-RUIZ, R. A. LIGERO and R. JIMENEZ-GARAY, *Mater. Lett.* **24** (1995) 287.
7. Y. B. LI, Q. YU, B. Q. WEI, J. LIANG and D. H. WU, *J. Mater. Sci. Lett.* **17** (1998) 607.
8. M. ENDO, K. TAKEUCHI, S. IGARASHI, K. KOBORI, M. SHIRAISHI and H. W. KROTO, *Carbon* **33** (1995) 873.
9. K. HERNADI, A. FONSECA, J.B. NAGY, D. BERNAERTS and A. A. LUCAS, *Carbon* **34** (1996) 1249.
10. J. P. ISSI, L. LANGER, J. HEREMANS and C. H. OLK, *Carbon* **33** (1995) 941.
11. T. W. EBBESEN, H. J. LEZEC, H. HIURA, J. W. BENNEIT, H. F. GHAEMI and T. THIO, *Nature* **382** (1996) 54.